

Citation for published version: Wang, X, Wilson, P, Leite, R, Chen, G, Freitas, H, Asadi, K, Smits, E, Katsouras, I & Rocha, P 2020, 'An Energy Harvester for Low-Frequency Electrical Signals', *Energy Technology*, vol. 8, no. 6, 2000114. https://doi.org/10.1002/ente.202000114

DOI:

10.1002/ente.202000114

Publication date: 2020

Document Version Peer reviewed version

Link to publication

This is the peer reviewed version of the following article: Wang, X., Wilson, P.R., Leite, R.B., Chen, G., Freitas, H., Asadi, K., Smits, E.C.P., Katsouras, I. and Rocha, P.R.F. (2020), An Energy Harvester for LowFrequency Electrical Signals. Energy Technol.. which has been published in final form at https://doi.org/10.1002/ente.202000114. This article may be used for non-commercial purposes in accordance with Wiley Terms and Conditions for Self-Archiving.

University of Bath

Alternative formats

If you require this document in an alternative format, please contact: openaccess@bath.ac.uk

Copyright and moral rights for the publications made accessible in the public portal are retained by the authors and/or other copyright owners and it is a condition of accessing publications that users recognise and abide by the legal requirements associated with these rights.

Take down policy
If you believe that this document breaches copyright please contact us providing details, and we will remove access to the work immediately and investigate your claim.

Download date: 07 Mar 2023



An energy harvester for low frequency electrical signals

Xin Wang^{[a], [b]}, Peter R. Wilson^[a], Ricardo B. Leite^[c], Guiyou Chen^[b], Helena Freitas^[d], Kamal Asadi^[e], Edsger C.P. Smits^[f], Ilias Katsouras^[f] and Paulo R.F. Rocha^{[a]*}

((Optional Dedication))

[a] Xin Wang, Prof. Peter R. Wilson, Dr. Paulo R. F. Rocha Centre for Biosensors, Bioelectronics and Biodevices (C3Bio) and Department of Electronic and Electrical Engineering, University of Bath, Claverton Down, Bath, BA2 7AY, United Kingdom.

E-mail: P.Rocha@bath.ac.uk

- [b] Xin Wang, Prof. Guiyou Chen School of Control Science and Engineering, Shandong University, Jinan, 250061, China.
- [c] Dr. Ricardo B. Leite Instituto Gulbenkian de Ciência, Rua da Quinta Grande nº6, 2780-343, Oeiras, Portugal.
- [d] Prof. Helena Freitas Centre for Functional Ecology - Science for People & the Planet, Department of Life Sciences, University of Coimbra, 3000-456 Coimbra, Portugal
- [e] Dr. Kamal Asadi Humboldt Research Group, Max Planck Institute for Polymer Research, Ackermannweg 10, 55128, Mainz, Germany
- [f] Dr. Edsger C.P. Smits, Dr. Ilias Katsouras Holst Centre, TNO- The Dutch Organization for Applied Scientific Research, High Tech Campus 31, 5656 AE Eindhoven, The Netherlands

Keywords: bioelectronics, triboelectric, triboelectricity, energy harvesting

Generating electricity from low frequency mechanical agitations produced by ocean waves, plants, or human motion is emerging as a key, environmentally-friendly technology in combating harmful emissions caused by burning fossil fuels. The generated electric pulses by the appropriate transducers, such as triboelectric or piezoelectric generators, need to be rectified and stored in a sustainable external circuit. The bottleneck, however, is the harvesting circuitry, which mostly relies on rather expensive up-conversion oscillation technologies. Such circuits are primarily

This article has been accepted for publication and undergone full peer review but has not been through the copyediting, typesetting, pagination and proofreading process, which may lead to differences between this version and the <u>Version of Record</u>. Please cite this article as <u>doi: 10.1002/ente.202000114</u>.

designed and optimized for frequencies well-above the kHz range, much higher than the aforementioned mechanical stimuli, and are therefore energy demanding. Here, we have developed a sustainable energy harvester that alleviates the need for using up-conversion and allows for efficient harvesting of the energy from low-frequency voltage pulses, as the ones typically generated by triboelectric or piezoelectric generators. Our resonant circuit has been designed to match the overall response originating from such low-frequency oscillating energy sources. Our design enables the harvester to be operable at frequencies as low as 1 Hz. We demonstrate CAD simulations, a miniaturized harvester on a printed-circuit-board using low-cost components, and discuss the scalability of the proposed design, which paves the way to affordable, efficient and sustainable low-cost energy solutions.

1. Introduction

Alternative renewable energy sources seek to scavenge various forms of energy from the environment. Established renewable-based energy technologies driven by natural energy, such as wind and solar are key approaches towards decarbonizing our energy system. However, the intermittent output of these sources is incompatible with energy consumers' needs. Even when state-of-the-art energy storage solutions become available, the energy system would still require substantial fossil-based generation as a back-up. Hence, to overcome the limitation of intermittency and the overwhelming dependence on fossil-based energy generation, new sources, such as triboelectric and piezoelectric generators, are emerging, as discussed extensively in the seminal work of Wang. These environmentally-friendly generators convert the low-frequency mechanical agitations from ocean waves are energingly into low-frequency alternating electric signals for energy harvesters. Although the average signal frequency feeding the harvester is about 1 Hz, the wave's unpredictable and non-periodic nature can lead to intervals ranging from 0.3 Hz to 300 Hz. The low output power varies from 700 μW to 20 mW. The low output power varies from 700 μW to 20 mW.



Scalable and efficient circuits to interface with low-frequency generators and increase output power are therefore needed.^[11]

Furthermore, plants have also been reported to produce oscillating and low-frequency electrical signals. The electric double layer formed by an insulating plant leaf cuticle (from a Rhododendron) and the adjacent conductive cellular tissue has been shown to possess triboelectric properties, where the low-frequency and alternating output power on a single leaf, upon a given force (0.9 N) reached about 15 µW cm⁻². Lab-scale set-ups in whole plants are producing an output power between 200 mW m⁻² and 500 mW m⁻². The alternating output power in plants has been reported to oscillate between 0.01 Hz and 10 Hz. In fact, microscopically, the existence of electrically excitable plants associated with environmental stress and stimuli has been investigated, even when no external force is applied. Plants such as *Mimosa pudica*, *Helianthus annuus* or *Dionaea muscipula* make use of ion channels to transmit information over long distances. In Plants, themselves, translate external stimuli into electrical signals, In as a survival mechanism and communication strategy. In resemblance to an electrical conducting cable, ion gradients across the plant tissue rapidly convey signals over long distances. Hence, plants communicate electrically, In In gradients and low-frequency signals.

Harvesting energy from low-frequency sources, particularly in the Hz regime, is technically challenging. State-of-the-art solutions to harvest low-frequency signals mostly rely on mechanical structure designs, [8b, 8i, 19] where up-conversion oscillation technologies play an important role. Several up-conversion methodologies that convert low-frequency ambient vibrations to higher frequency oscillations via a piezoelectric beam generator have been developed. [20] Yet, these technologies tend to be expensive to manufacture, and unreliable in the long term due to cantilever

impact degradation.^[20] The up-conversion process itself is prone to energy losses, which are detrimental to the output power efficiency.

In this work, we have developed a technology to harvest energy from low-frequency sources, eliminating the need for up-conversion techniques. The resonant circuit frequency of our harvester has been modelled and matched to the low-frequency oscillating energy source. We demonstrate an energy harvester prototype, based on an optimized LTC3108 on a miniaturized PCB, which comprises a step-up transformer and a boost converter, to condition and harvest the alternating signals prevenient from a low-frequency pulse train. All considered, this work paves the way for efficient energy harvesting circuits from a variety of low-frequency, green energy sources.

2. Experimental

The energy harvester PCB prototype depicted in Figure 1(a) was designed by using the electronic design automation tool Altium Designer 18.1.7. To minimize the PCB size, the surface-mount variant of all necessary electronic components was selected. PCB trace dimensions were determined using the IPC-2221 standard. PCBs were fabricated using 35 μ m copper thickness and 1.6 mm of glass re-enforced Fr-4. The PCB was populated with a Coilcraft LPR6235-752SMR transformer, with a primary inductance of 7.5 μ H, a measured secondary coil inductance of 63.56 mH and an inter-winding capacitance of 62.8 pF. The boost converter used was the LTC3108 from Analog Devices, with an SSOP16 footprint and buffer with reference MAX9650. The LTC3108 peripheral capacitors, namely $C_{\rm res}$, $C_{\rm cp}$ and $C_{\rm byp}$, used SMD 0805 footprints. The capacitance values were 10 μ F, 620 pF and 2.2 μ F, respectively. A polarized tantalum SMD capacitor from AVX, with a value of 1000 μ F, was employed as the storage capacitor, $C_{\rm store}$. The integrated circuit uses a charge pump approach to power conversion and has been implemented in a PCB. The schematic of the complete circuit is given in Supplementary Figure S1. The miniaturized circuit has a total area of less than 9



cm². Inductance and capacitance measurements were performed using a TENMA 72-10465 LCR Meter.

All simulations were performed using the LTspice[®] and SaberTM software suites. Small-signal analysis was simulated in SaberTM using a 50 mV peak voltage input. The output voltage over time was simulated using the behavioural model in the time domain, utilizing a 1 Hz pulse train.

The experimental characterization of the PCB prototype was carried out using a 33210A Pulse Generator, from Keysight Technologies, with a programmed input stimulus in the form of periodic square wave pulses, or pulse train. The schematic of the circuit used to determine the V-I power curve is depicted in Figure 1(b). The minimum voltage, current and power required for the harvester to operate, was determined by setting the signal generator to output a 1 Hz, 50 % duty cycle square wave with a 20 Ohm internal load. Varying the resistance of the potentiometer, R_p , then results in the power curve shown in Figure 1(c). The input power was calculated as:

$$P = \frac{1}{2} \cdot V \cdot I\#(1)$$

Figure 1(c) shows that for the targeted low frequency input of 1 Hz square pulses, the circuit requires a minimum input power of 180 μ W, which corresponds to a minimum voltage magnitude of 36 mV. The optimized harvester topology and circuit parameters leading to the power curve depicted in Figure 1(c) are explained in the next sections.

3. Results

3.1. Resonant Circuit

The energy harvester comprises a resonant circuit and a state-of-the-art LTC3108 boost converter, for harvesting energy from an ultra-low input voltage source, below 50 mV. Typically, resonant circuits focus on harvesting high-frequency signals, in the kHz regime. Conventional ranges are This article is protected by copyright. All rights reserved

essentially between 10 kHz and 100 kHz. The resonant circuit used with the LTC3108 is depicted in Figure 2(a). The low-frequency input signal, $V_{\text{res-in}}$, is fed into the resonant circuit through a load impedance stabilizer, constructed by MAX9650. The resonant circuit includes the internal N-Channel MOSFET switch of the LTC3108, the inductance of the secondary winding of the transformer, L_{sec} , and the input capacitance, C_{res} . In order to form a close-loop and stabilize the circuit, the primary winding of the transformer is connected to the drain of the N-Channel MOSFET, namely the SW pin, as suggested by the manufacturer. [22]

The resonant circuit uses an external step-up transformer with a turn's ratio of 100, in order to increase the voltage. The frequency of oscillation, f_{res} , is determined by L_{sec} and C_{res} . The oscillation frequency^[22] and relation between the L_{sec} and C_{res} is given by Equation 2:

$$f_{\rm res} = \frac{1}{2\pi \cdot \sqrt{L_{\rm sec} \cdot C_{\rm res}}} \Leftrightarrow C_{\rm res} = \frac{1}{f_{\rm res}^2 \cdot 4\pi^2 \cdot L_{\rm sec}} \#(2)$$

3.2. Boost Converter

The architecture of the LTC3108 is shown in Figure 2(b) and in more detail in Supplementary Figure S1. The output voltage from the resonant circuit stage ($V_{\text{res-out}}$) can be coupled to the charge-pump and rectifier circuit inside the LTC3108, using the capacitor C_{cp} . This enables the output voltage to be harvested. The output voltage of the LTC3108 is configured to be 3.1 V by connecting pin VS₁ to VAUX, VS₂ to ground and bypassing the VAUX by a 2.2 μ F capacitor C_{byp} . An energy storage capacitor C_{out} is used to store the output energy. Another large capacitor, C_{store} , is also connected from pin V_{store} to ground, to power the system in the event the input voltage is lost. This capacitor will be charged to the maximum VAUX clamp voltage, which is 3.1 V for this design. We note that the energy harvester used in this work was designed to provide an output voltage up to 3.1 V; the integrated circuit can also be configured to provide a programmable target output of 2.5 V, 4.1 V or 5.0 V.



Considering both the input power level from triboelectric generators and the design requirements of the energy harvesting circuit, the value of capacitors C_{byp} , C_{out} and C_{store} were chosen as 2.2 μ F, 220 μ F and 1000 μ F, respectively.

3.3. Low Frequency Matching

The frequency of the signals generated by triboelectric generators and plants is typically in the range of a few Hz. To allow the electronics to decode and efficiently harvest such low-frequency signals, the resonant circuit needs to be designed to match the overall response originating from these low-frequency oscillating energy sources.

There is a constraint on the circuit resonant component that needs to be taken into account. The value of the secondary inductance has an upper limit, due to a practical size limitation of the inductor with increasing number of turns. Moreover, the concomitant increase in winding resistance would introduce a high level of loss into the circuit. Given this constraint, the value of $L_{\rm sec}$ was chosen and measured to be 63 mH. This value is based on a primary theoretical inductance of 7.5 μ H and a turn's ratio of 1:100. Note that it is not unusual for tolerances of 10-20 % to occur in magnetic components due to the intrinsic variability of the permeability of the magnetic material in the core.

The signal frequency generated by triboelectric sources, including plants, varies between 0.3 Hz and 300 Hz^[7a, 7b, 10]. Assuming a resonant frequency of 200 Hz, Equation 2 leads to a C_{res} of 10 μ F. Therefore, this value was used instead of the 330 pF, mentioned in the application example described in the LTC3108 datasheet, henceforth referred to as "default".

Empirical testing of the energy harvesting circuit established that the capacitance value of the input capacitor for the energy harvesting circuit, C_{cp} , is proportional to the one of the resonant capacitor,

This article is protected by copyright. All rights reserved



 C_{res} . It should therefore be similarly scaled, resulting in a desired value of 680 pF. However, we need to consider the parallel inter-winding parasitic capacitance of 62.8 pF, which needs to be subtracted from the scaled C_{cp} . Hence, the final value of C_{cp} was set to 620 pF, which is the nearest standard value to the desired 617.2 pF.

3.4. Simulation and Experimental Validation of the Frequency Matching Effect

To understand the effect of $C_{\rm res}$ and $L_{\rm sec}$ on the resonant frequency, we performed a simulation analysis using a small-signal model. Note that we did not use switching electronics to enable small-signal frequency analysis, instead we used an averaged model of the boost converter that allows direct frequency analysis. The small-signal model used is a linearized power switch model of the form described by Middlebrook, which is established as a method for obtaining accurate frequency responses of switching power regulators. The model uses an averaged model of the power-switching stage to obtain a linear model that reflects the overall frequency domain behaviour of the power converter. The model is linear in nature and can, therefore, be used to calculate the small-signal frequency response directly, without the need for non-linear algorithms, such as Newton-Raphson. It is also common to express the output in decibels (dB), rather than in absolute voltage. For unity gain, the resulting output would be 1 V or 0 dB. Therefore, positive gain is larger than 0 dB and negative gain is smaller than 0 dB.

Simulations were carried out to establish a suitable set of circuit parameters, ensuring the optimal compromise between circuit efficiency and availability of hardware. As discussed in the low frequency matching section, the optimum value for the secondary inductance and capacitance of the resonant circuit, are approximately 63 mH and 10 μ F, respectively.

To optimize the energy harvester circuit, we performed a frequency response analysis, while tuning the transformer primary inductance, L_p . In Figure 3(a) we show gain as a function of frequency for This article is protected by copyright. All rights reserved

different values of the inductance, ranging between 75 nH and 7.5 μ H, while using the default value, 330 pF, for $C_{\rm res}$. A shift from 10^2 Hz to 10^0 Hz, for 0 dB is observed. An improved performance over the frequency range from 0.3 Hz to 300 Hz is notable, albeit with a gain still attenuated at low frequencies. We can conclude that simply using the default value for the boost converter, viz. $C_{\rm res}$ = 330 pF and $L_{\rm p}$ = 75 nH, does not yield an effective response, as the gain is negative in the low frequency regime. We therefore performed, in Figure 3(b), the small-signal simulation as a function of the other resonant parameter, $C_{\rm res}$. The inductance, $L_{\rm p}$, was fixed to 7.5 μ H. The resonant parameter $C_{\rm res}$ was varied from the default value of 330 pF to 10 μ F. Increasing $C_{\rm res}$ enabled positive gain at low frequencies. In fact, the positive gain or 0 dB mark, shifts 5 orders of magnitude, from 10^5 Hz to 10^0 Hz, enabling harvesting at low frequency.

Increasing $C_{\rm res}$ to the calculated optimal value of 10 μ F, resulted in a bandwidth improvement at the lower frequency end. Yet, increasing $C_{\rm res}$ has its limits. We experimentally verified that there is a practical limit of around 10 μ F before the circuit performance begins to degrade, possibly due to magnetic saturation of the Ferrite-based transformer and circuit parasitics, such as the stray capacitance between the transformer windings and wire resistance in the circuit.

Hence, we determine that for the energy harvester to operate in the lowest possible regime, the resonating capacitor needs to be 10 μ F, and the related $C_{\rm cp}$ needs to be 620 pF. Supplementary Figure S2 shows the effect of varying $C_{\rm cp}$ on the output voltage.

3.5. Low Frequency Characterization of the Energy Harvester

The charging process of the output capacitor C_{out} , depicted in Figure 2(b), can be represented as output voltage over time, and therefore serves as the performance indicator of the energy harvester. Figure 3(c) depicts, in green, the simulated output voltage of the default harvester that is not optimized for low frequency. In this case no output voltage is generated. The notable effect of

matching the circuit resonant frequency to lower input frequencies can be seen in the simulation represented in red, where $C_{\text{res}}=10 \ \mu\text{F}$. In less than 1 minute, the output voltage rises from 0 V to 3 V.

Figure 3(c) shows the actual experimental response of a prototype harvester to a low-frequency signal of 1 Hz, using the minimum input signal magnitude of 36 mV, as determined from the data in Figure 1(c). The measured output voltage is presented by the solid blue line. The output voltage reaches a value of 3.1 V within 80 s. The input power scales up to 1 mW, limited by the internal storage capacity of the boost converter.

The output was further characterized as a function of the input signal amplitude, duty cycle and inter-pulse interval, as shown in Figure 4. Figure 4(a) shows the output voltage over time, for different input voltages. For Figure 4(a-c), the first measurement point represents the minimum conditions for the harvester to operate and charge the output capacitor C_{out} . Increasing the amplitude from 36 mV to typical voltages recorded in plants, i.e., 100 mV, [14] the harvester is able to reach the peak voltage of 3.1 V within less than 10 s, for a 1 Hz square pulse. In addition to varying the input magnitude, we also varied the duty cycle. Figure 4(b) shows the output voltage over time for different intervals of the input square wave, or pulse train. The duty cycle varies from 35 % to 80 %. The frequency is fixed at 1 Hz. For a minimum duty cycle of 35 %, the harvester charges up C_{out} , and within 250 s reaches the maximum voltage of 3.1 V. Increasing the duty cycle to 80 % enables the harvester to reach 3.1 V in 25 s. Finally, due to the unpredictable nature of waves and plants' electrogenecity, the output voltage over time is characterized as a function of the inter-pulse intervals. The inter-pulse interval between two consecutive square wave peaks was varied from 1 s to 3 s. The pulse width was fixed at 0.5 s. As shown in Figure 4(c), even for peaks at 3 s apart, the harvester is able to output about 2.2 V within 400 s. As the inter-pulse decreases, the charging of C_{out} is faster. At a 1 s inter-pulse interval, the harvester reaches the maximum output

of 3.1 V in less than 1 minute. Note that these results are for the minimum input voltage of 36 mV. Increasing the input voltage to typical recorded spikes in plants, *i.e.* 100 mV, increases the interpulse intervals, at which the harvester can realistically be used, to several seconds. As an example, an output voltage of 2.5 V is reached within 150 s, even when using a 100 mV low-frequency pulse with an inter-pulse interval of 10 s, as shown in Figure 4(d). Hence, within the aforementioned boundary conditions, the circuit can also handle non-periodic input signals.

4. Summary and Conclusion

We demonstrated an energy harvester optimized to operate in the low-frequency regime. The energy harvester consists of a step-up transformer in series with a boost converter, whose input resonant frequency has been matched to that of typical triboelectric generators and electrogenic plants. Our design is validated both by simulations and by experimentally characterizing a homemade, miniaturized, prototype PCB. By optimizing the resonant circuit, the positive gain at low frequencies shifts 5 orders of magnitude, from 10⁵ Hz to 10⁰ Hz, when compared to a default and state-of-the-art boost converter. Our miniaturized prototype enables harvesting of alternating electric signals, with frequencies as low as 0.1 Hz.

The topology allows scalability, *i.e.* multiple harvesting circuits can be cascaded to the specified bus voltage of a local energy system such as 400 V, based on a standard PV facility, and ultimately connected to the grid.

Supporting Information

Supporting Information is available from the Wiley Online Library or from the author.

Acknowledgements

We would like to thank Sivapathasundaram Sivaraya, Michael Linham and David Chapman for technical support. We acknowledge the financial support from the University of Bath and from the Alexander von Humboldt Foundation (Germany) through the Sofja Kovalevskaja Award, as well as the support from the Max-Planck Institute for Polymer Research.

Received: ((will be filled in by the editorial staff))
Revised: ((will be filled in by the editorial staff))
Published online: ((will be filled in by the editorial staff))



References

- [1] aZ. L. Wang, Advanced Materials 2012, 24, 280-285; bC. Dagdeviren, Z. Li, Z. L. Wang, Annual Review of Biomedical Engineering 2017, 19, 85-108; cZ. L. Wang, J. Chen, L. Lin, Energy & Environmental Science 2015, 8, 2250-2282; dJ. Chen, Z. L. Wang, Joule 2017, 1, 480-521; eS.-M. Xu, X. Liang, X.-Y. Wu, S.-L. Zhao, J. Chen, K.-X. Wang, J.-S. Chen, Nature Communications 2019, 10, 1-10; fK. Liu, B. Kong, W. Liu, Y. Sun, M.-S. Song, J. Chen, Y. Liu, D. Lin, A. Pei, Y. Cui, Joule 2018, 2, 1857-1865; gJ. Wan, J. Xie, X. Kong, Z. Liu, K. Liu, F. Shi, A. Pei, H. Chen, W. Chen, J. Chen, Nature nanotechnology 2019, 14, 705-711.
- [2] aG. Zhu, J. Chen, T. Zhang, Q. Jing, Z. L. Wang, *Nature communications* **2014**, *5*, 3426; bB. Zhang, J. Chen, L. Jin, W. Deng, L. Zhang, H. Zhang, M. Zhu, W. Yang, Z. L. Wang, *ACS nano* **2016**, *10*, 6241-6247; cL. Zhang, B. Zhang, J. Chen, L. Jin, W. Deng, J. Tang, H. Zhang, H. Pan, M. Zhu, W. Yang, *Advanced Materials* **2016**, *28*, 1650-1656; dY. Yang, G. Zhu, H. Zhang, J. Chen, X. Zhong, Z.-H. Lin, Y. Su, P. Bai, X. Wen, Z. L. Wang, *ACS nano* **2013**, *7*, 9461-9468; eJ. Chen, J. Yang, H. Guo, Z. Li, L. Zheng, Y. Su, Z. Wen, X. Fan, Z. L. Wang, *ACS nano* **2015**, *9*, 12334-12343.
- [3] aN. Zhang, F. Huang, S. Zhao, X. Lv, Y. Zhou, S. Xiang, S. Xu, Y. Li, G. Chen, C. Tao, *Matter* **2020**; bL. Zheng, G. Cheng, J. Chen, L. Lin, J. Wang, Y. Liu, H. Li, Z. L. Wang, *Advanced Energy Materials* **2015**, *5*, 1501152.
- [4] aD. Y. Leung, Y. Yang, Renewable and Sustainable Energy Reviews **2012**, *16*, 1031-1039; bS. Mekhilef, R. Saidur, A. Safari, Renewable and sustainable energy reviews **2011**, *15*, 1777-1790.
- [5] T. Adefarati, R. Bansal, IET Renewable Power Generation 2016, 10, 873-884.
- [6] Z. L. Wang, G. Zhu, Y. Yang, S. Wang, C. Pan, *Materials today* **2012**, *15*, 532-543.
- [7] aU. T. Jurado, S. H. Pu, N. M. White, *IEEE Sensors Journal* **2019**; bX. Wang, S. Niu, Y. Yin, F. Yi, Z. You, Z. L. Wang, *Advanced Energy Materials* **2015**, *5*, 1501467; cJ. Chen, J. Yang, Z. Li, X. Fan, Y. Zi, Q. Jing, H. Guo, Z. Wen, K. C. Pradel, S. Niu, *ACS nano* **2015**, *9*, 3324-3331; dG. Zhu, Y. Su, P. Bai, J. Chen, Q. Jing, W. Yang, Z. L. Wang, *ACS nano* **2014**, *8*, 6031-6037; eY. Su, X. Wen, G. Zhu, J. Yang, J. Chen, P. Bai, Z. Wu, Y. Jiang, Z. L. Wang, *Nano Energy* **2014**, *9*, 186-195; fQ. Jing, G. Zhu, P. Bai, Y. Xie, J. Chen, R. P. Han, Z. L. Wang, *ACS nano* **2014**, *8*, 3836-3842.
- [8] aQ. Guan, G. Lin, Y. Gong, J. Wang, W. Tan, D. Bao, Y. Liu, Z. You, X. Sun, Z. Wen, *Journal of Materials Chemistry A* **2019**, *7*, 13948-13955; bJ. Chen, G. Zhu, W. Yang, Q. Jing, P. Bai, Y. Yang, T. C. Hou, Z. L. Wang, *Advanced materials* **2013**, *25*, 6094-6099; cL. Jin, J. Chen, B. Zhang, W. Deng, L. Zhang, H. Zhang, X. Huang, M. Zhu, W. Yang, Z. L. Wang, *ACS nano* **2016**, *10*, 7874-7881; dW. Yang, J. Chen, G. Zhu, J. Yang, P. Bai, Y. Su, Q. Jing, X. Cao, Z. L. Wang, *ACS nano* **2013**, *7*, 11317-11324; eG. Zhu, P. Bai, J. Chen, Z. L. Wang, *Nano Energy* **2013**, *2*, 688-692; fT.-C. Hou, Y. Yang, H. Zhang, J. Chen, L.-J.

- Chen, Z. L. Wang, *Nano Energy* **2013**, *2*, 856-862; gZ. Lin, J. Chen, X. Li, Z. Zhou, K. Meng, W. Wei, J. Yang, Z. L. Wang, *ACS nano* **2017**, *11*, 8830-8837; hP. Bai, G. Zhu, Z.-H. Lin, Q. Jing, J. Chen, G. Zhang, J. Ma, Z. L. Wang, *ACS nano* **2013**, *7*, 3713-3719; iJ. Yang, J. Chen, Y. Yang, H. Zhang, W. Yang, P. Bai, Y. Su, Z. L. Wang, *Advanced Energy Materials* **2014**, *4*, 1301322; jC. Yan, Y. Gao, S. Zhao, S. Zhao, Y. Zhou, W. Deng, Z. Li, G. Jiang, L. Jin, G. Tian, *Nano Energy* **2020**, *67*, 104235; kK. Meng, S. Zhao, Y. Zhou, Y. Wu, S. Zhang, Q. He, X. Wang, Z. Zhou, W. Fan, X. Tan, *Matter* **2020**.
- [9] aJ. Chen, Y. Huang, N. Zhang, H. Zou, R. Liu, C. Tao, X. Fan, Z. L. Wang, *Nature Energy* **2016**, *1*, 16138; bS. Niu, X. Wang, F. Yi, Y. S. Zhou, Z. L. Wang, *Nature communications* **2015**, *6*, 8975.
- [10] aU. T. Jurado, S. H. Pu, N. M. White, in 2017 IEEE SENSORS, IEEE, 2017, pp. 1-3; bZ. Li, Z. Saadatnia, Z. Yang, H. Naguib, Energy conversion and management 2018, 174, 188-197; cS. Kim, S. J. Choi, K. Zhao, H. Yang, G. Gobbi, S. Zhang, J. Li, Nature communications 2016, 7, 10146; dJ. Chun, B. U. Ye, J. W. Lee, D. Choi, C.-Y. Kang, S.-W. Kim, Z. L. Wang, J. M. Baik, Nature communications 2016, 7, 12985.
- [11] aL. Dhakar, S. Gudla, X. Shan, Z. Wang, F. E. H. Tay, C.-H. Heng, C. Lee, *Scientific reports* **2016**, 6, 22253; bX. Li, Y. Sun, *IEEE Transactions on Power Electronics* **2019**.
- [12] M. Helder, D. Strik, H. Hamelers, A. Kuhn, C. Blok, C. Buisman, *Bioresource technology* **2010**, *101*, 3541-3547.
- [13] F. Meder, I. Must, A. Sadeghi, A. Mondini, C. Filippeschi, L. Beccai, V. Mattoli, P. Pingue, B. Mazzolai, *Advanced Functional Materials* **2018**, 28, 1806689.
- [14] J. Fromm, S. Lautner, *Plant, cell & environment* **2007**, *30*, 249-257.
- [15] aA. Christmann, E. Grill, *Nature* **2013**, *500*, 404; bS. A. Mousavi, A. Chauvin, F. Pascaud, S. Kellenberger, E. E. Farmer, *Nature* **2013**, *500*, 422.
- [16] aR. Hedrich, V. Salvador-Recatalà, I. Dreyer, *Trends in Plant Science* **2016**, *21*, 376-387; bP. R. Rocha, A. D. Silva, L. Godinho, W. Dane, P. Estrela, L. K. Vandamme, J. B. Pereira-Leal, D. M. De Leeuw, R. B. Leite, *Scientific reports* **2018**, *8*, 5484.
- [17] A. G. Volkov, *International Journal of Parallel, Emergent and Distributed Systems* **2017**, 32, 44-55.
- [18] aE. Davies, in *Plant electrophysiology*, Springer, **2006**, pp. 407-422; bA. Falciatore, M. R. d'Alcalà, P. Croot, C. Bowler, *Science* **2000**, 288, 2363-2366; cH. Awan, R. S. Adve, N. Wallbridge, C. Plummer, A. W. Eckford, *IEEE transactions on nanobioscience* **2018**, *18*, 61-73; dE. D. Brenner, R. Stahlberg, S. Mancuso, J. Vivanco, F. Baluška, E. Van Volkenburgh, *Trends in plant science* **2006**, *11*, 413-419.
- [19] aH. Zhang, Y. Yang, Y. Su, J. Chen, K. Adams, S. Lee, C. Hu, Z. L. Wang, *Advanced Functional Materials* **2014**, *24*, 1401-1407; bW. Yang, J. Chen, G. Zhu, X. Wen, P. Bai, Y. Su, Y. Lin, Z. Wang, *Nano Research* **2013**, *6*, 880-886.
- [20] M. Safaei, H. A. Sodano, S. R. Anton, Smart Materials and Structures 2019, 28, 113001.
- [21] The Institute for Interconnecting and Packaging Electronic Circuits (IPC), in *IPC-2221*, Association Connecting Electronics Industries, **1998**.
- [22] Analog Devices Inc., LTC3108 Ultralow Voltage Step-Up Converter and Power Manager Datasheet., **2010**.
- [23] aV. Vorpérian, *IEEE Transactions on aerospace and electronic systems* **1990**, 26, 497-505; bR. D. Middlebrook, S. Cuk, in *1976 IEEE Power Electronics Specialists Conference*, IEEE, **1976**, pp. 18-34.

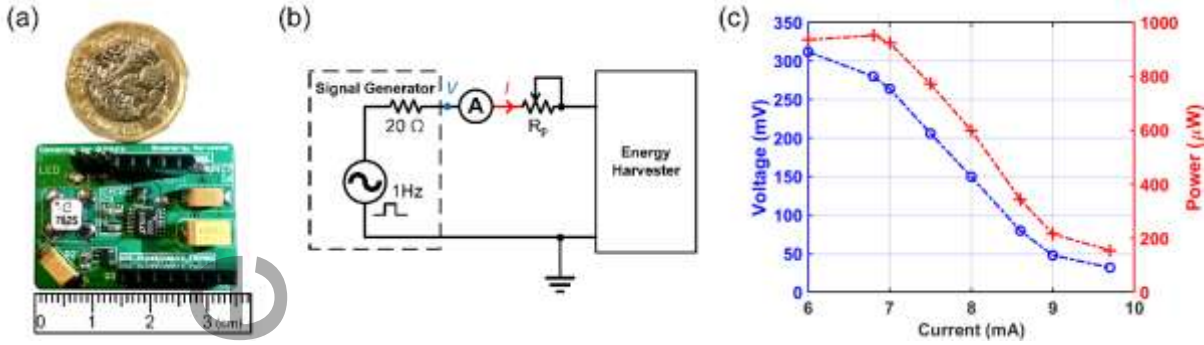


Figure 1. (a) The miniaturized prototype PCB. A ruler and a one-pound sterling coin are shown as a scale reference. (b) Schematic of the V-I curve test circuit. (c) Minimum voltage, current and power for the harvester prototype to operate with an input square wave with a frequency of 1 Hz and a 50% duty cycle.

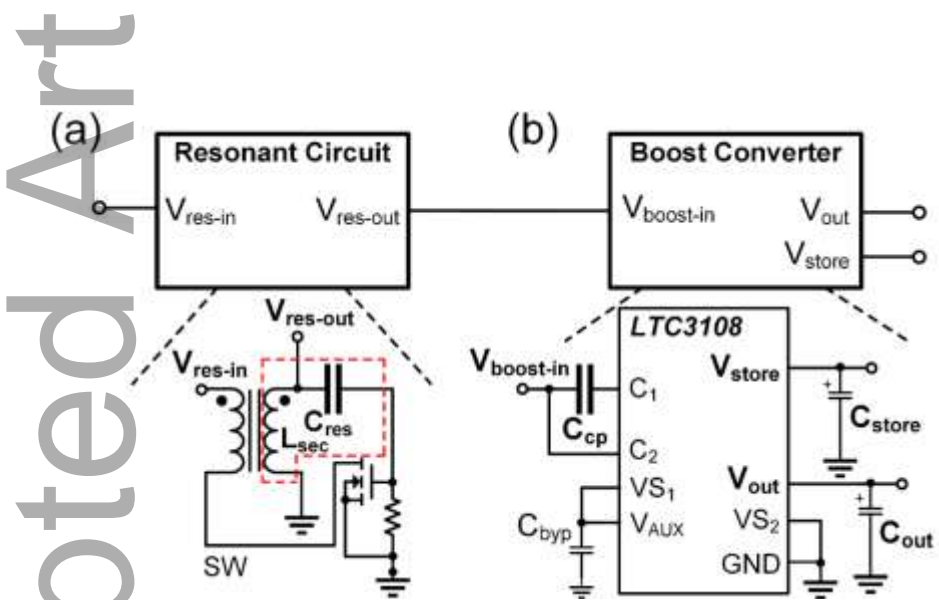


Figure 2. Overall energy harvester architecture showing (a) the resonant circuit and (b) the LTC3108 boost converter.

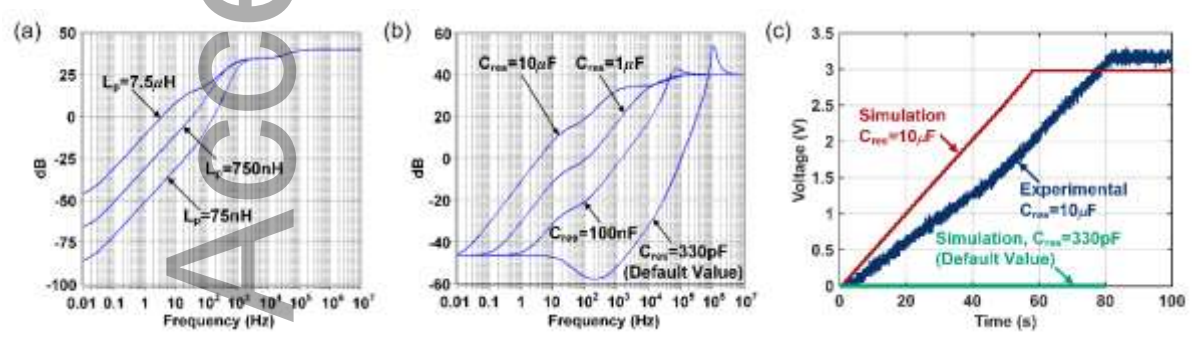


Figure 3. (a) Harvester output amplitude as a function of frequency, while varying the transformer primary inductance, $L_{\rm p}$, from 75 nH to the optimized 7.5 μ H, with the default value of 330pF for the resonant capacitor, $C_{\rm res}$. (b) Frequency response analysis of the energy harvester circuit while tuning the resonant capacitor, $C_{\rm res}$, from the default 330 pF to the optimized value of 10 μ F. (c) Simulated (red) and experimental (blue) output voltage using a 1 Hz input pulse train with 25 mV amplitude for the simulations and 36 mV for the experimental validation. The green trace represents the default LTC3108 simulation, which yields no output. The values for $C_{\rm cp}$ and $C_{\rm res}$ were 620 pF and 10 μ F, respectively.

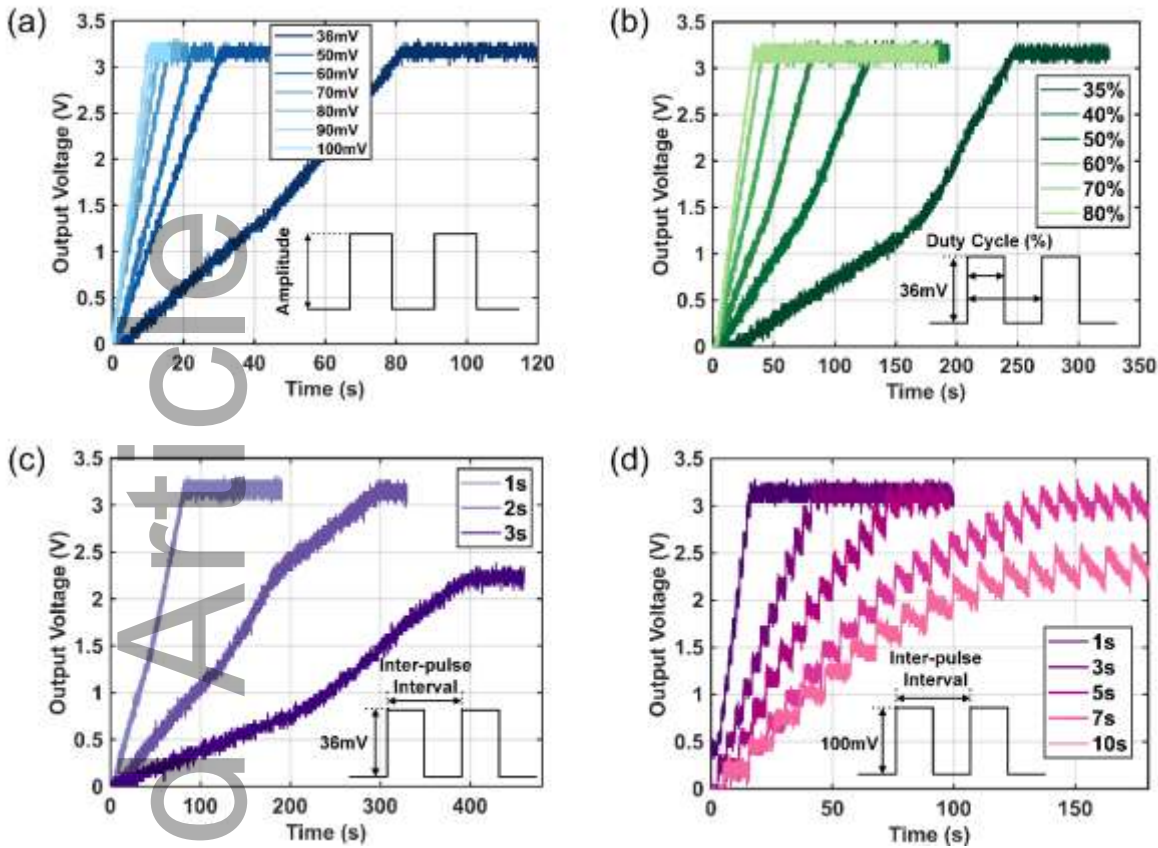


Figure 4. PCB prototype characterization. Output voltage over time: (a) varying the input amplitude from 36 mV to 100 mV. The frequency of the input signal was fixed at 1 Hz. The inset illustrates the input signal parameter being changed; (b) varying the duty cycle of the input square wave from 35 % to 80 %, at a fixed input frequency of 1 Hz; (c) varying the inter-pulse interval between two consecutive square wave peaks, from 1 s to 3 s. The pulse width was fixed at 0.5 s and the amplitude was fixed at 36 mV; (d) varying the inter-pulse interval between two consecutive square wave peaks from 1 s to 10 s. The pulse width was fixed at 0.5 s and the amplitude was fixed at 100 mV.

Keyword: Energy Harvesting

Xin Wang, Peter R. Wilson, Ricardo B. Leite, Guiyou Chen, Helena Freitas, Kamal Asadi, Edsger C.P. Smits, Ilias Katsouras and Paulo R.F. Rocha*

An energy harvester for low frequency electrical signals

ed Article

TOC

We devised a technology to harvest energy from low frequency sources, eliminating the need for up-conversion techniques. We accomplish this by modelling and tuning the resonant frequency of an energy harvesting system, which comprises a step-up transformer and a boost converter on a miniaturized PCB prototype.

